# Application of Nanosecond Pulsed Electric Fields into He La Cells Expressing Enhanced Green Fluorescent Protein and Fluorescence Lifetime Microscopy

**ARTICLE** *in* THE JOURNAL OF PHYSICAL CHEMISTRY B · AUGUST 2012

Impact Factor: 3.3 · DOI: 10.1021/jp306550v · Source: PubMed



**3 AUTHORS**, INCLUDING:

Kamlesh Awasthi
National Chiao Tung University
**19** PUBLICATIONS **47** CITATIONS

SEE PROFILE

THE JOURNAL OF PHYSICAL CHEMISTRY B

Article

pubs.acs.org/JPCB

# Application of Nanosecond Pulsed Electric Fields into HeLa Cells Expressing Enhanced Green Fluorescent Protein and Fluorescence Lifetime Microscopy

Kamlesh Awasthi, Takakazu Nakabayashi, and Nobuhiro Ohta*

Research Institute for Electronic Science (RIES), Hokkaido University, Sapporo 001-0020, Japan

**ABSTRACT:** An electrode microchamber has been constructed for applying nanosecond pulsed strong electric fields to living cells, and fluorescence lifetime microscopy (FLIM) has been used to investigate the effects of external electric fields on dynamics and function of HeLa cells expressing enhanced green fluorescent protein (EGFP). Both morphological change in cells and reduction of the fluorescence lifetime of EGFP have been observed after application of electric fields having a pulsed width of 50 ns and a strength of 4 MV $m^{-1}$, indicating that apoptosis, which is a programmed cell death, was induced by nanosecond pulsed electric fields and that fluorescence lifetime of EGFP decreased along with the induction of apoptosis. The reduction of the fluorescence lifetime occurred before the morphological change, indicating that FLIM provides a sensitive and noninvasive detection of the progress of apoptosis induced by application of nanosecond pulsed electric fields.

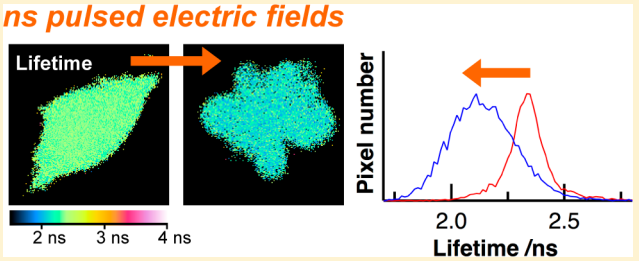


## INTRODUCTION

Application of external electric fields has been extensively used in variety fields of science and technology. In a field of bio and medical sciences, electric fields have widely been used to modulate membrane permeabilization, called electroporation.[1−3] Exposure of living cells to electric fields causes accumulation of electric charges at the plasma membrane, resulting in the reversible rearrangement of the plasma membrane with formation of pores or aqueous channels. Such alteration with electric fields induces temporary increase in the membrane permeability, which has been used to deliver extracellular compounds, including pharmacological and genetic materials, into cells. It has also been reported that irradiation of high-intensity near-infrared femtosecond laser pulses at the cell membrane induces the transient increase in the membrane permeability through which DNA could enter.[4]

In electroporation with pulsed electric fields having a duration of 0.1−10 ms and strengths of orders of kV $cm^{-1}$, applied electric fields accumulate ions along the plasma membrane, causing a counter field inside the cell. The generated counter field shields intracellular compartments from the applied electric field, resulting in the pore formation in the plasma membrane. With application of short and pulsed electric fields of the nanosecond time scale, on the other hand, it has been pointed out that intracellular membranes may be affected without any significant effect on the plasma membrane.[5−8] When the pulsed electric field is applied to cells with duration below the charging time of the plasma membrane, for example, it has been suggested that applied electric fields can penetrate into a cell before the charge dissipation into the plasma membrane, charging organelle membranes such as the nuclear envelope. This may allow modulating intracellular structure, dynamics, and function without physical damage of the plasma membrane. Actually, the distinct effects of nanosecond pulsed electric fields on cells have been compared with conventional plasma membrane electroporation,[5,9−11] and application of nanosecond pulsed electric fields to cells was reported to induce tumor growth inhibition,[11,12] calcium bursts,[10,13,14] nuclear perturbation,[14,15] and apoptosis.[11,12,16−18] It has also been reported that the probability of subcellular effects increases and that of plasma membrane effects decreases, as the duration of pulsed electric fields is decreased.[15]

We have constructed an experimental system of a time-resolved fluorescence lifetime microscopy (FLIM) and studied cellular environments and physiological parameters of a cell.[19−24] Intensity imaging of fluorescence microscopy has widely been applied for measuring subcellular structures and localization of fluorescent dyes in a living cell. However, fluorescence intensity can vary, depending on the experimental condition, and quantitative evaluation of fluorescence intensity is very difficult in some cases. In contrast, fluorescence lifetime, which is one of the inherent properties of a dye, is independent of dye concentration, photobleaching, and excitation intensity but dependent on ion concentrations and local environments surrounding fluoropores. This makes FLIM a powerful method for performing quantitative analysis of environments and molecular dynamics inside a cell.[25−29]

In the present study, we have constructed an electrode microchamber for applying nanosecond pulsed electric fields to

**Received:** July 2, 2012
**Revised:** August 14, 2012
**Published:** August 16, 2012

living systems and measured the images both of the fluorescence intensity and of the fluorescence lifetime of HeLa cells expressing enhanced green fluorescent protein (EGFP) before and after exposure to nanosecond pulsed electric fields. It has been shown that apoptosis is induced by the present nanosecond pulsed electric fields and that the fluorescence lifetime of EGFP is changed in association with field-induced apoptosis process.

Apoptosis is the natural process of programmed cell death in which cells activate an intracellular death program and kill themselves in a controlled way.[30−32] Apoptosis is distinguished by a set of characteristic morphological changes including cell shrinkage and membrane blebbing. The major signaling pathways for apoptosis are the extrinsic death receptor and the intrinsic mitochondrial pathways, both of which result in the activation of a family of cysteinyl aspartate-specific proteases, called caspases, which has been considered as central, indispensable executioners of apoptosis.[33] Apoptosis plays a crucial role in development of cellular organisms, and understanding of the mechanism of apoptosis is significant not only for clarifying the regulation of tissue development and differentiation but also for developing techniques and therapeutic agents for the prevention and treatment of many diseases such as cancer. Cancer cells have an ability to evade apoptotic death, and a large number of researchers have devoted themselves to the development of chemotherapeutic drugs and radiation treatments for induction of apoptosis in cancer cells.[34,35] Application of nanosecond pulsed electric fields is a unique method to induce apoptosis so quickly, and the present study shows that FLIM is useful to investigate the primary process of the field-induced apoptosis.

## EXPERIMENTAL SECTION

**Electrode Microchamber.** We have constructed a microchamber by a photolithography method for observing cell response to intense nanosecond voltage pulses. The schematic image of the setup of the microchamber and its electrode pattern are shown in Figure 1. Living cells in the spacing of the Au electrodes of ca. 0.1 mm can be observed in vivo with an inverted confocal microscope. The fabrication of the microchamber is as follows. Cover glasses rinsed thoroughly with acetone and methanol were etched in buffered oxide etchant for 5−7 min at room temperature and baked at 120 °C for 20 min. SU-8 2015 negative photoresist (Micro Chem) was spun on the etched substrate at 500 rpm for 35 s and 2500 rpm for 30 s and then prebaked at 95 °C for 3 min. The prebaked substrate was exposed to UV light through the mask pattern for the electrode (Figure 1B) for 35 s and postbaked at 95 °C for 2 min and then developed in 2-methoxy-1-methylethyl acetate (Wako). By this procedure, a chamber having a sharply defined edge and smooth vertical side wall could be made. The three-dimensional microchamber was then formed with side walls of ∼20 μm.

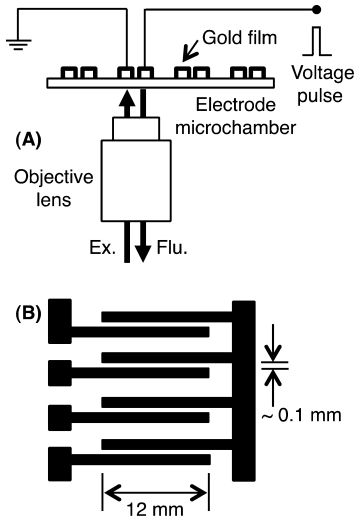


**Figure 1.** (A) Schematic representation of the setup of the electrode microchamber. (B) Top view of the fabricated four-channel gold electrodes on a cover glass.

The deposition of metal films was carried out as follows. Positive photoresist ZEP520 (ZEONREX Electronic Chemicals) was spun on the three-dimensional chamber at 500 rpm for 5 s and 2500 rpm for 30 s and then baked at 120 °C for 2 min. The resulting substrate was exposed to UV light through the same mask as that used for SU-8 2015 negative photoresist for 10 s, resulting in the complementary structure in which ZEP520 covered the areas outside the electrode areas of SU-8 2015. Then Ti and Au layers were deposited on the photoresist microchamber by helicon sputtering (MPS-4000C1/HC1, ULVAC). The Ti and Au layers were 10 and 35 nm, respectively, in thickness. The Ti layer was used to improve the adhesion of gold to the photoresist microchamber. The sputtering of each metal was carried out twice at +30° and −30°, respectively, with respect to the substrate to cover the sidewalls. After the deposition of the metal films, the substrate was baked from room temperature to 120 °C. The melting of ZEP520 releases the metal film from undesired areas of the substrate. Finally, the resultant electrode microchamber was immersed in acetone for 10−15 min. The ultrasonic treatment was also used to clean the substrate.

Nanosecond pulsed electric fields were generated in the electrode microchamber by a homemade pulse generator. The 50 ns pulsed voltage with a strength of 400 V could be applied to a load resistance of 50 Ω, which corresponds to the field strength of 4 MV $m^{-1}$ for the interelectrode distance of 0.1 mm.

**Cell Culture.** HeLa cells were cultured in Dulbecco's modified Eagle's medium (DMEM, D5796, Sigma) supplemented with 2 × $10^5$ U $dm^{-3}$ penicillin G, 200 mg of streptomycin sulfate, and 10% of fetal bovine serum. HeLa cells were incubated in humidified atmosphere containing 5% $CO_2$ at 37 °C. The incubated cells were transfected overnight with plasmid DNA encoding EGFP using Optifect Transfection Reagent (12579-017, Invitrogen) in the electrode microchamber. The medium was replaced with phenol red free Opti-MEM I reduced serum medium just before the FLIM measurement, which is mentioned below.

In the measurements of fluorescence intensity image of annexinV-FITC, the annexin V assay was carried out by using an annexin V-FITC apoptosis kit (Clontech). The annexin V-FITC positive cells were observed by fluorescence microscopy before and after application of nanosecond pulsed electric fields.

**FLIM Measurements.** Measurements of fluorescence lifetime image were carried out using a four-channel time-gated detection method.[19−24] The second harmonic of the output from a mode-locked Ti:sapphire laser (Tsunami, Spectra Physics, pulse duration of about 80 fs, repetition rate of 81 MHz) was used as an excitation light source. The excitation beam was introduced into a scanner head (Digital Eclipse C1,


dx.doi.org/10.1021/jp306550v | J. Phys. Chem. B 2012, 116, 11159−11165

Nikon) and focused onto cells in the electrode microchamber placed on the stage of an inverted microscope (TE2000E, Nikon) through the objective lens (40×). Fluorescence from the cells was collected by the same objective lens and entered into interference filters to select the wavelength of emission. The fluorescence signal was detected by a photomultiplier in a high-speed lifetime imaging module (LIMO, Nikon Europe BV). Fluorescence decays were measured at each pixel of the image, and the lifetime imaging module captured the fluorescence decay trace into four time windows. The fluorescence lifetime at each pixel of the image was evaluated from the four time-window signals by assuming a single exponential decay, and the results were converted into a fluorescence lifetime image. All of the time windows were set at 2.0 ns. The excitation wavelength was 440 nm, and the fluorescence in the region of 515−560 nm was detected.

## RESULTS AND DISCUSSION

Figure 2 shows the representative fluorescence intensity and fluorescence lifetime images of a single HeLa cell expressing

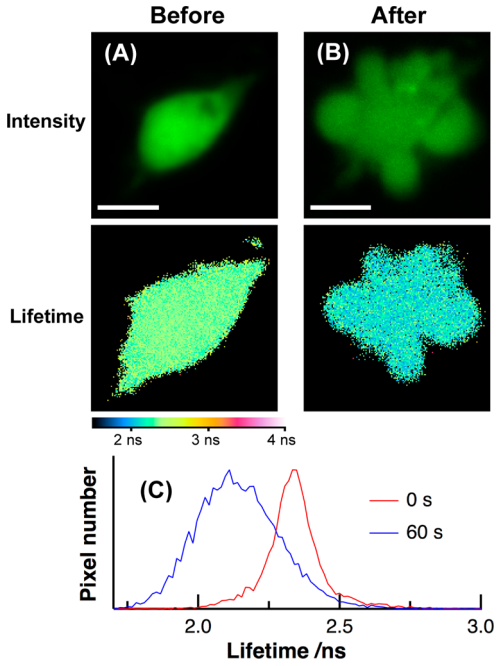


**Figure 2.** Fluorescence intensity image (upper) and corresponding fluorescence lifetime image (lower) of a HeLa cell expressing EGFP before (A) and after (B) application of pulsed electric fields of 4 MV $m^{-1}$ at 1 kHz for 60 s. The pulse duration was 50 ns. The histograms of the fluorescence lifetime of the images of (A) and (B) are shown in (C). Scale bars in (A) and (B) are 20 $\mu$m.

EGFP before and after application of nanosecond pulsed electric fields. The fluorescence arises from EGFP inside a cell, and the green shape in the intensity image represents a single HeLa cell expressing EGFP. The corresponding lifetime image of the cell is shown just under the intensity image. The images of the same cell were compared before and after application of electric fields. It is seen that application of pulsed electric fields (pulse width of 50 ns, field strength of 4 MV $m^{-1}$, frequency of 1 kHz, application time of 60 s) induced a change in cell morphology. The observed cell membrane blebbing shown in Figure 2B is related to cell death through apoptosis, indicating that the nanosecond pulsed electric fields induce apoptotic cell

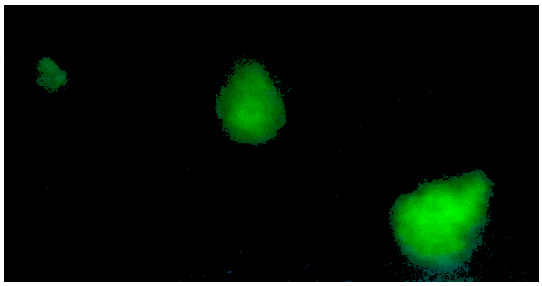

**Figure 3.** Fluorescence intensity image of annexin V-FITC in HeLa cells observed after 180 s application of nanosecond pulsed electric fields with a frequency of 1 kHz.

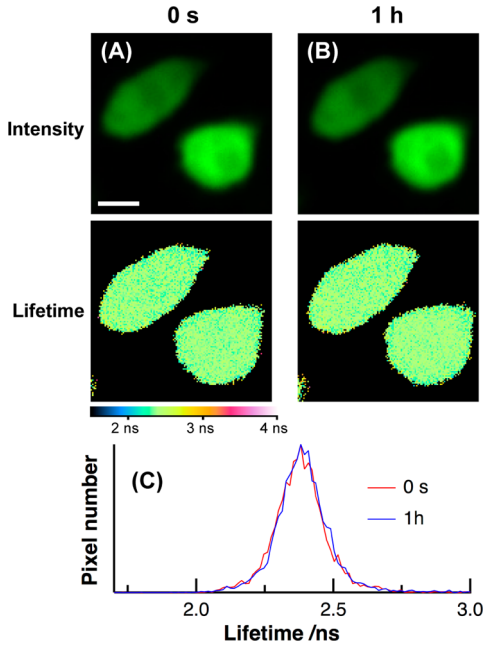


**Figure 4.** Fluorescence intensity image (upper) and corresponding fluorescence lifetime image (lower) of HeLa cells expressing EGFP with a time lapse of 0 (A) and 1 h (B). Pulsed electric fields were not applied to these cells. The histograms of the fluorescence lifetime of the images of (A) and (B) are shown in (C). Scale bar in (A) is 20 $\mu$m.

death. Membrane permeabilization due to applied electric fields appears to be insufficient to induce apoptosis in cells,[36,37] and short nanosecond and strong pulsed electric fields are mandatory for HeLa cells to sufficiently induce apoptosis. The fluorescence lifetime image also exhibited the change in the fluorescence lifetime with application of pulsed electric fields, as shown in Figure 2. The fluorescence lifetime of a HeLa cell expressing EGFP was reduced by application of nanosecond pulsed electric fields, which is clearly shown in the histograms of the fluorescence lifetime. The peak of the histogram was at 2.3 ns before the application, which became shorter to be at 2.1 ns after the application. Thus, the lifetime decreased by a factor of about 10% with application of electric fields, as shown in Figure 2.

The loss of plasma membrane asymmetry is one of the key features of the early stage of apoptosis, and the redistribution of phosphatidylserin (PS) to the outer layer of plasma membrane is usually detected through apoptosis with annexin V that has strong affinity for PS.

As shown in Figure 3, staining of annexin V-FITC, which exhibits PS redistribution, was observed with application of


dx.doi.org/10.1021/jp306550v | J. Phys. Chem. B 2012, 116, 11159−11165

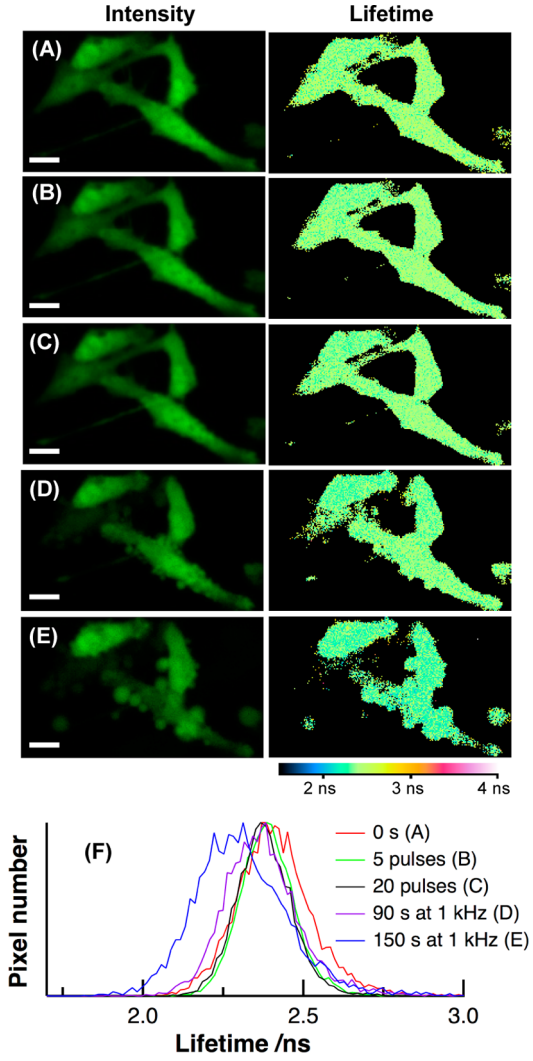


**Figure 5.** Fluorescence intensity and corresponding fluorescence lifetime images of HeLa cell expressing EGFP before (A) and after application of 5 (B) and 20 (C) nanosecond pulses of 4 MV $m^{-1}$. The images of the same cells after application of 4 MV $m^{-1}$ at 1 kHz for 90 and 150 s are shown in (D) and (E), respectively. The pulse duration was 50 ns. The histograms of the fluorescence lifetime of the images of (A)−(E) are shown in (F). Scale bars are 20 $\mu$m.

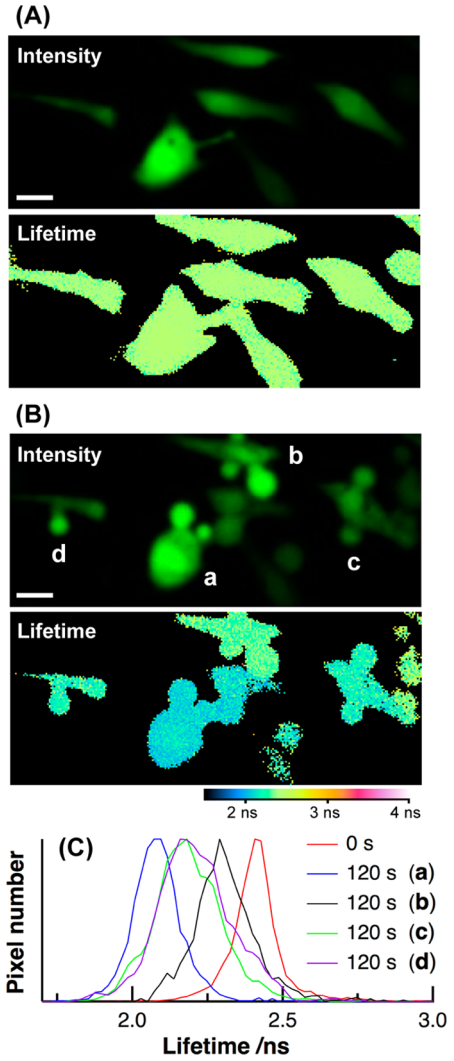


**Figure 6.** Fluorescence intensity and corresponding fluorescence lifetime images of HeLa cell expressing EGFP before (A) and after (B) application of pulsed electric fields of 4 MV $m^{-1}$ at 1 kHz for 120 s. The pulse duration was 50 ns. The histograms of the fluorescence lifetime of the cell labeled **a**−**d** in the intensity image of (B) and that of all the cells before application of pulsed electric fields of the image (A) are shown in (C). Scale bars are 20 $\mu$m. Electric field was applied along the vertical direction.

nanosecond pulsed electric field having a pulse width of 50 ns and a field strength of 4 MV $m^{-1}$, indicating the loss of the plasma membrane asymmetry through the nanosecond pulsed electric-field-induced apoptosis.

To confirm the electric field effect on fluorescence lifetime, time-lapse measurements of the fluorescence images of HeLa cells expressing EGFP were performed without application of electric fields. The representative time-lapse images in the absence of electric fields are shown in Figure 4. The changes in morphology and in fluorescence lifetime were not observed without application of electric fields even after an interval of 1 h, indicating that the observed changes in Figure 2 were induced by application of pulsed electric fields. Note that the FLIM measurements were done with above-mentioned microchambers in both cases.

In the present experiments, autofluorescence was negligible because the dull nucleus was not observed in the intensity images.[24,38] It is worth mentioning that the intensity of autofluorescence in nuclei is much weaker than that in other areas, resulting in the dull nucleus region in autofluorescence images. Apoptosis induces a change in intracellular environment such as shift in cellular redox state and change in ion concentration and the decrease in the fluorescence lifetime; i.e., the increase of the nonradiative process at the emitting state with pulsed electric fields may be ascribed to a change in protein structure or protein environment during field-induced apoptosis. The green fluorescence of GFP is known to arise from the anionic form of the chromophore identified as a structure of *p*-hydroxybenzylidene−imidazolidinone, which is located near the center of the can-shaped tertiary structure.[39,40] The chromophore of GFP is rigidly encapsulated inside the protein structure and is surrounded by both apolar and polar residues, including some charged residues, all of which produce an electrostatic field to the chromophore. The chromophore structure and the protein environment surrounding the chromophore are responsible for optical properties of GFP.[41,42] The present results suggest that apoptotic process


dx.doi.org/10.1021/jp306550v | J. Phys. Chem. B 2012, 116, 11159−11165

caused by nanosecond pulsed electric fields induces environmental changes surrounding the GFP chromophore, resulting in the reduction of the fluorescence lifetime. It can therefore be said that FLIM provides sensitive and noninvasive detection of apoptosis, which induces changes in environments surrounding the GFP chromophore. It is unlikely that denaturation occurs after the application of nanosecond pulsed electric fields, since more drastic reduction of the fluorescence lifetime is expected for denaturated proteins.[43,44]

Steric and electrostatic effects of the protein structure govern the value of the fluorescence lifetime of the GFP chromophore. The steric hindrance of the protein structure significantly inhibits the nonradiative structural relaxation of the chromophore,[43,44] and electric fields produced by charged and polar groups in the protein structure affect the chromophore photophysics.[45,46] In fact, we have previously shown that application of electric fields induces a change in the fluorescence lifetime of the encapsulated chromophore in a fluorescent protein;[47] however, it should be noted that much stronger electric fields than the one used in the present study are necessary to induce the lifetime change, indicating that the present lifetime change is induced by field-induced changes in environments of EGFP. It is therefore conceivable that the field-induced apoptotic process induces a slight structural change as well as a change of local field in EGFP, which results in the reduction of the observed fluorescence lifetime. This means that the changes in the protein structure due to the field-induced apoptosis enhance the nonradiative decay rate of the anionic form of the EGFP chromophore.

The refractive index around GFP is the important factor that affects the fluorescence lifetime of GFP. It was shown that the lifetime of GFP after photoexcitation of the anionic chromophore varied with the square of the refractive index of the bulk solvent, as expected from the equation for a radiative decay rate constant.[48] The fluorescence lifetime of GFP fusion protein was used to evaluate the local refractive index of GFP in a cell.[49] Recently, the change in the fluorescence lifetime of GFP in HeLa cells was observed during mitosis, which was ascribed to changes in the refractive index around GFP.[50] The alteration of the refractive index was considered to result from changes in concentration of macromolecules in the cell interior during the cell cycle progression. As described above, the fluorescence lifetime of GFP was found to be shortened by application of electric fields,[47] and we consider a slight structural change of the protein structure of GFP, which leads to a change of local field, as the origin of the change in fluorescence lifetime after application of nanosecond pulsed electric fields. However, we have to confess that we cannot flatly reject the possibility that the present lifetime change arises from changes in refractive index inside a cell. The fluorescence quantum yield of GFP is about 0.6,[42] indicating that fluorescence lifetime as well as fluorescence quantum yield is determined by both radiative decay rate and nonradiative decay rate. If the lifetime shortening results from the change in refractive index, i.e., from the enhancement of the radiative decay rate, the fluorescence quantum yield is expected to increase. If the change in lifetime results from the enhancement of the nonradiative decay rate, on the other hand, fluorescence quantum yield is expected to decrease. If both fluorescence lifetime and quantum yield can be measured before and after application of nanosecond pulsed electric fields, this problem can be made clear. At the moment, however, it is very difficult to evaluate the change in fluorescence quantum yield, which will be a future problem.

We have previously examined the relationship between the fluorescence lifetime of EGFP and apoptosis and measured the time course of fluorescence lifetime images as well as fluorescence intensity images of HeLa cells expressing EGFP after induction of apoptosis with an apoptosis inducer (tumor necrosis factor-$\alpha$ (TNF-$\alpha$) in combination with cycloheximide (CHX)).[23] The decrease of the fluorescence lifetime was observed along with a morphological change, indicating that the reduction of the fluorescence lifetime of EGFP is related with changes in cellular environments with apoptosis. The reduction of the lifetime due to acidic environment is enhanced with the excitation wavelength around 400 nm that excites the neutral species of the EGFP chromophore.[20,51] The magnitude of the lifetime decrease, however, remained constant with the excitation wavelengths of 405 and 440 nm, indicating that the observed apoptosis-induced change in lifetime did not come from the pH dependence.[23] It is worth mentioning that apoptosis can be quickly induced by nanosecond pulsed electric fields. Such a quick induction of apoptosis without any reagents is expected to be used in a variety of biomedical applications. Cell membrane blebbing that is one of the key features of apoptosis occurs less than 60 s in the presence of nanosecond pulsed electric fields with a time duration of 50 ns (Figure 2), while the induction time of several hours was necessary to observe cell membrane blebbing after adding TNF-$\alpha$/CHX.

We have also measured the dependence of the fluorescence intensity and lifetime images of HeLa cells on the number of applied voltage pulses. Both images of HeLa cells expressing EGFP after the exposure to 5 and 20 voltage pulses are shown in Figures 5B and 5C, respectively. Both images observed before the application of electric field are also shown in Figure 5A. Note that the same cells were monitored to observe morphology as well as lifetime as a function of the number of applied voltage pulses. As shown in Figures 5A–C, application of only several voltage pulses did not induce apparent morphological changes in cell, but a discernible change in the fluorescence lifetime of EGFP was observed. Figure 5F shows the histograms of the fluorescence lifetime images measured with different number of applied voltage pulses. The histogram of the lifetime before the application of electric field exhibited a peak at around 2.4 ns, and the lifetime histogram became narrower in a longer lifetime region after application of 5 and 20 pulses with a remaining peak of 2.4 ns. As mentioned above, the fluorescence lifetime remained unchanged without application of electric fields even after an interval of 1 h (see Figure 4), indicating that the observed lifetime change was induced by application of voltage pulses. The observed change in lifetime probably reflects the change in cellular environments following the application of electric fields. As shown in Figure 5, cell membrane blebbing occurred after the exposure to nanosecond pulsed electric fields of 4 MV $m^{-1}$ at 1 kHz for 90 s. The peak of the lifetime histogram shifted to a shorter lifetime, as the number of the applied voltage pulses increases, e.g., around 2.25 ns for 150 s (see Figure 5F).

It should be noted that the magnitudes of the field-induced changes both in the morphology and in the lifetime depend on the size and physical conditions of cells and their alignments between the electrodes even with the same strengths of the applied electric field. Figure 6 shows the fluorescence intensity and corresponding fluorescence lifetime images of HeLa cells expressing EGFP before and after application of nanosecond

pulsed electric fields. The morphological change due to pulsed electric fields was observed in all the cells (Figure 6B). The fluorescence lifetime of each cell was also reduced with pulsed electric fields. However, the magnitudes of the lifetime reduction were different from each other. After the application of pulsed electric fields, the cell labeled **a** exhibits a peak of the histogram of the lifetime at around 2.1 ns, while the cell labeled **b** exhibits a peak at around 2.3 ns (see Figure 6C). Note that all the cells in the image exhibit almost the same fluorescence lifetime before the application of electric fields, i.e., 2.4 ns. Thus, the progress of the field-induced apoptosis, which can be controlled by changing parameters of pulse duration, repetition rate, amplitude voltage, or exposure time, can be clarified from the magnitude of the fluorescence lifetime reduction.

In conclusion, fluorescence intensity and lifetime images of HeLa cells expressing EGFP have been measured with and without application of nanosecond pulsed electric fields with a time duration of 50 ns and a field strength of 4 MV $m^{-1}$. Morphological changes due to apoptosis were observed with application of the pulsed electric fields. The fluorescence lifetime of EGFP was also found to decrease in association with a field-induced apoptosis process, which is ascribed to the change in environments surrounding the chromophore of EGFP. The fact that the field-induced change in fluorescence lifetime is observed following application of nanosecond pulsed voltage, even when the morphological change is not confirmed, suggests that FLIM is useful to investigate apoptosis, that is, to pursue the progress of the apoptosis induced by application of ultrashort pulsed electric fields.

## AUTHOR INFORMATION

### Corresponding Author

*E-mail: nohta@es.hokudai.ac.jp.

### Notes

The authors declare no competing financial interest.

## ACKNOWLEDGMENTS

We are grateful to Dr. Fan Sun and Prof. Masataka Kinjo at Hokkaido University for helping with preparation of HeLa cells expressing EGFP. This work was supported in part by a Grant-in-Aid for Scientific Research (Grant No. 20245001) from the Ministry of Education, Culture, Sports, Science and Technology in Japan.

## REFERENCES

(1) Zimmermann, U.; Pilwat, G.; Riemann, F. *Biophys. J.* **1974**, *14*, 881−899.
(2) Kinosita, K., Jr.; Ashikawa, I.; Saita, N.; Yoshimura, H.; Itoh, H.; Nagayama, K.; Ikegami, A. *Biophys. J.* **1988**, *53*, 1015−1019.
(3) Dev, S. B.; Rabussay, D. P.; Widera, G.; Hofmann, G. A. *IEEE Trans. Plasma Sci.* **2000**, *28*, 206−223.
(4) Tirlapur, U. K.; König, K. *Nature* **2002**, *418*, 290−291.
(5) Schoenbach, K. H.; Katsuki, S.; Stark, R. H.; Buescher, E. S.; Beebe, S. J. *IEEE Trans. Plasma Sci.* **2002**, *30*, 293−300.
(6) Sun, Y.; Vernier, P. T.; Behrend, M.; Marcu, L.; Gundersen, M. A. *IEEE Trans. Nanobiosci.* **2005**, *4*, 277−283.
(7) Schoenbach, K. H.; Xiao, S.; Joshi, R. P.; Camp, J. T.; Heeren, T.; Kolb, J. F.; Beebe, S. J. *IEEE Trans. Plasma Sci.* **2008**, *36*, 414−422.
(8) Tang, L.; Yao, C.; Sun, C. *Biochem. Biophys. Res. Commun.* **2009**, *390*, 1098−1101.
(9) Deng, J.; Schoenbach, K. H.; Buescher, E. S.; Hair, P. S.; Fox, P. M.; Beebe, S. J. *Biophys. J.* **2003**, *84*, 2709−2714.
(10) Vernier, P. T.; Sun, Y.; Marcu, L.; Salemi, S.; Craft, C. M.; Gundersen, M. A. *Biochem. Biophys. Res. Commun.* **2003**, *310*, 286−295.
(11) Beebe, S. J.; White, J.; Blackmore, P. F.; Deng, Y.; Somers, K.; Schoenbach, K. H. *DNA. Cell Biol.* **2003**, *22*, 785−796.
(12) Beebe, S. J.; Fox, P. M.; Rec, L. J.; Somers, K.; Stark, R. H.; Schoenbach, K. H. *IEEE Trans. Plasma Sci.* **2002**, *30*, 286−292.
(13) White, J. A.; Blackmore, P. F.; Schoenbach, K. H.; Beebe, S. J. *J. Biol. Chem.* **2004**, *279*, 22964−22972.
(14) Sun, Y.; Vernier, P. T.; Behrend, M.; Wang, J.; Thu, M. M.; Gundersen, M.; Marcu, L. *J. Biomed. Opt.* **2006**, *11*, 024010.
(15) Chen, N.; Schoenbach, K. H.; Kolb, J. F.; Swanson, R. J.; Garner, A. L.; Yang, J.; Joshi, R. P.; Beebe, S. J. *Biochem. Biophys. Res. Commun.* **2004**, *317*, 421−427.
(16) Hall, E. H.; Schoenbach, K. H.; Beebe, S. J. *Apoptosis* **2007**, *12*, 1721−1731.
(17) Mi, Y.; Yao, C.; Li, C.; Sun, C.; Tang, L.; Liu, H. *IEEE Trans. Dielectr. Electr. Insul.* **2009**, *16*, 1302−1310.
(18) Ford, W. E.; Ren, W.; Blackmore, P. F.; Schoenbach, K. H.; Beebe, S. J. *Arch. Biochem. Biophys.* **2010**, *497*, 82−89.
(19) Wang, H.-P.; Nakabayashi, T.; Tsujimoto, K.; Miyauchi, S.; Kamo, N.; Ohta, N. *Chem. Phys. Lett.* **2007**, *442*, 441−444.
(20) Nakabayashi, T.; Wang, H.-P.; Kinjo, M.; Ohta, N. *Photochem. Photobiol. Sci.* **2008**, *7*, 668−670.
(21) Nakabayashi, T.; Nagao, I.; Kinjo, M.; Aoki, Y.; Tanaka, M.; Ohta, N. *Photochem. Photobiol. Sci.* **2008**, *7*, 671−674.
(22) Nakabayashi, T.; Wang, H.-P.; Tsujimoto, K.; Miyauchi, S.; Kamo, N.; Ohta, N. *Chem. Lett.* **2008**, *37*, 522−523.
(23) Ito, T.; Oshita, S.; Nakabayashi, T.; Sun, F.; Kinjo, M.; Ohta, N. *Photochem. Photobiol. Sci.* **2009**, *8*, 763−767.
(24) Ogikubo, S.; Nakabayashi, T.; Adachi, T.; Islam, Md. S.; Yoshizawa, T.; Kinjo, M.; Ohta, N. *J. Phys. Chem. B* **2011**, *115*, 10385−10390.
(25) Wallrabe, H.; Periasamy, A. *Curr. Opin. Biotechnol.* **2005**, *16*, 19−27.
(26) Becker, W.; Bergmann, A.; Biskup, C. *Microsc. Res. Tech.* **2007**, *70*, 403−409.
(27) Levitt, J. A.; Matthews, D. R.; Ameer-Beg, S. M.; Suhling, K. *Curr. Opin. Biotechnol.* **2009**, *20*, 28−36.
(28) Berezin, M. Y.; Achilefu, S. *Chem. Rev.* **2010**, *110*, 2641−2684.
(29) Borst, J. W.; Visser, A. J. W. G. *Meas. Sci. Technol.* **2010**, *21*, 102002.
(30) Allen, R. T.; Hunter, W. J., III; Agrawal, D. K. *J. Pharmacol. Toxicol. Methods* **1997**, *37*, 215−228.
(31) Nagata, S. *Cell* **1997**, *88*, 355−365.
(32) Green, D. R.; Reed, J. C. *Science* **1998**, *281*, 1309−1312.
(33) Earnshaw, W. C.; Martins, L. M.; Kaufmann, S. H. *Annu. Rev. Biochem.* **1999**, *68*, 383−424.
(34) Makin, G.; Dive, C. *Trends Cell Biol.* **2001**, *11*, S22−S26.
(35) Brown, J. M.; Attardi, L. D. *Nat. Rev. Cancer* **2005**, *5*, 231−237.
(36) Li, L. H.; Sen, A.; Murphy, S. P.; Jahreis, G. P.; Fuji, H.; Hui, S. W. *Exp. Cell Res.* **1999**, *253*, 541−550.
(37) Gowrishankar, T. R.; Esser, A. T.; Vasilkoski, Z.; Smith, K. C.; Weaver, J. C. *Biochem. Biophys. Res. Commun.* **2006**, *341*, 1266−1276.
(38) Ostrander, J. H.; McMahon, C. M.; Lem, S.; Millon, S. R.; Brown, J. Q.; Seewaldt, V. L.; Ramanujam, N. *Cancer Res.* **2010**, *70*, 4759−4766.
(39) Ormö, M.; Cubitt, A. B.; Kallio, K.; Gross, L. A.; Tsien, R. Y.; Remington, S. J. *Science* **1996**, *273*, 1392−1395.
(40) Yang, F.; Moss, L. G.; Phillips, G. N., Jr. *Nat. Biotechnol.* **1996**, *14*, 1246−1251.
(41) Tsien, R. Y. *Annu. Rev. Biochem.* **1998**, *67*, 509−544.
(42) Zimmer, M. *Chem. Rev.* **2002**, *102*, 759−781.
(43) Webber, N. M.; Litvinenko, K. L.; Meech, S. R. *J. Phys. Chem. B* **2001**, *105*, 8036−8039.
(44) Kummer, A. D.; Kompa, C.; Niwa, H.; Hirano, T.; Kojima, S.; Michel-Beyerle, M. E. *J. Phys. Chem. B* **2002**, *106*, 7554−7559.
(45) Ohta, N. *Bull. Chem. Soc. Jpn.* **2002**, *75*, 1637−1655.

(46) Nakabayashi, T.; Hino, K.; Ohta, Y.; Ito, S.; Nakano, H.; Ohta, N. *J. Phys. Chem. B* **2011**, *115*, 8622−8626.
(47) Nakabayashi, T.; Kinjo, M.; Ohta, N. *Chem. Phys. Lett.* **2008**, *457*, 408−412.
(48) Suhling, K.; Siegel, J.; Phillips, D.; French, P. M. W.; Lévêque-Fort, S.; Webb, S. E. D.; Davis, D. M. *Biophys. J.* **2002**, *83*, 3589−3595.
(49) van Manen, H.-J.; Verkuijlen, P.; Wittendorp, P.; Subramaniam, V.; van den Berg, T. K.; Roos, D.; Otto, C. *Biophys. J.* **2008**, *94*, L67−L69.
(50) Pliss, A.; Zhao, L.; Ohulchanskyy, T. Y.; Qu, J.; Prasad, P. N. *ACS Chem. Biol.* **2012**, *7*, 1385−1392.
(51) Heikal, A. A.; Hess, S. T.; Webb, W. W. *Chem. Phys.* **2001**, *274*, 37−55.